

Article

Sustainable and Low-Cost Hemp FRP Composite Confinement of B-Waste Concrete

Panuwat Joyklad ¹, Ekkachai Yooprasertchai ^{2,*}, Abdur Rahim ³, Nazam Ali ⁴, Krisada Chaiyasarn ⁵ and Qudeer Hussain ⁶

- ¹ Department of Civil and Environmental Engineering, Faculty of Engineering, Srinakharinwirot University, Nakhonnayok 26120, Thailand; panuwatj@g.swu.ac.th
 - ² Construction Innovations and Future Infrastructure Research Center (CIFIR), Department of Civil Engineering, Faculty of Engineering, King Mongkut's University of Technology Thonburi, Bangkok 10140, Thailand
 - ³ Department of Transportation Engineering and Management, University of Engineering and Technology, Lahore 54890, Pakistan; rahim@uet.edu.pk
 - ⁴ Department of Civil Engineering, University of Management and Technology, Lahore 54770, Pakistan; nazam.ali@umt.edu.pk
 - ⁵ Thammasat Research Unit in Infrastructure Inspection and Monitoring, Repair and Strengthening (IIMRS), Thammasat School of Engineering, Faculty of Engineering, Thammasat University Rangsit, Pathum Thani 12000, Thailand; ckrisada@engr.tu.ac.th
 - ⁶ Center of Excellence in Earthquake Engineering and Vibration, Department of Civil Engineering, Chulalongkorn University, Bangkok 10330, Thailand; ebbadat@hotmail.com
- * Correspondence: ekkachai.yoo@kmutt.ac.th



Citation: Joyklad, P.; Yooprasertchai, E.; Rahim, A.; Ali, N.; Chaiyasarn, K.; Hussain, Q. Sustainable and Low-Cost Hemp FRP Composite Confinement of B-Waste Concrete. *Sustainability* **2022**, *14*, 7673. <https://doi.org/10.3390/su14137673>

Academic Editors: Libo Yan, Ruoyu Jin, Yidong Xu and Zhenhua Duan

Received: 12 May 2022

Accepted: 20 June 2022

Published: 23 June 2022

Publisher's Note: MDPI stays neutral with regard to jurisdictional claims in published maps and institutional affiliations.



Copyright: © 2022 by the authors. Licensee MDPI, Basel, Switzerland. This article is an open access article distributed under the terms and conditions of the Creative Commons Attribution (CC BY) license (<https://creativecommons.org/licenses/by/4.0/>).

Abstract: Each year, massive amount of construction waste is generated that needs proper attention in terms of its disposal without deteriorating surrounding environment. A significant portion of this waste comprises bricks. Besides, large number of new construction works are resulting in the depletion of natural resources rapidly. Intuitively, a sustainable solution demands to consume this construction waste in the best way possible. This study targeted brick waste as a potential material to be used as a partial replacement of natural aggregates in structural concrete. It has been known that the concrete constructed with recycled brick aggregates possesses substandard mechanical properties. Traditionally, synthetic FRPs are known to strengthen recycled aggregate concrete. However, recognizing high costs associated with them, this study proposed the use of natural hemp fiber ropes to strengthen recycled aggregate concrete constructed with brick aggregates. To assess the efficacy of hemp ropes in strengthening mechanical properties of the concrete with coarse aggregates partially replaced with recycled brick aggregates (B-waste), an experimental framework was conducted. Sixteen cylindrical specimens were tested in two groups depending upon the concrete strength. Within each group, 2 specimens each were strengthened with 1, 2, and 3 layers of hemp fiber ropes. Axial monotonic compressive loading was applied to each specimen. Results revealed that hemp fiber ropes significantly improved ultimate compressive strength and the corresponding strain. A substantial improvement in axial ductility was observed. For the sake of performance-based non-linear modelling, accurate constitutive modelling at material level is necessary. For this purpose, several existing analytical stress-strain models were tested in this study to predict ultimate confined compressive strength and strain. It was found that several models predicted confined compressive strengths with reasonable accuracy. However, very few models were able to predict confined peak strain with good accuracy.

Keywords: hemp fiber rope; recycled aggregate concrete; cement-clay interlocking brick aggregates; stress-strain models

1. Introduction

Concrete has been utilized in construction works for decades ascribing to its easy preparation, availability, and durability. It has been reported that concrete is the second

most used material on Earth after water. Roughly, up to three tonnes of concrete is used annually for each person [1]. Old concrete structures often require rehabilitation works or complete demolition to pave way for new constructions. This generates colossal concrete waste each year that requires proper disposal without leaving significant carbon footprints. For residential buildings and other low-rise structures, bricks are widely used and have been an important constituent. In addition, brickwork is often found in the construction of boundary walls of buildings (see Figure 1).



Figure 1. Use of cement clay interlocking bricks at Chachoengsao Province, Thailand (a) boundary wall, (b) walls and columns.

It has been reported that approximately 15.5 million tonnes of construction waste comprising concrete and bricks is produced annually in China [2]. The report of the European Union in 2011 concluded that approximately 1 billion tons of construction and demolition waste is produced in the European Union annually with bricks as a key component [3]. Production of huge waste each year in combination with quick depletion of natural resources have resulted in natural urge to reuse in construction works. A critical query arises probing the impact of recycled brick aggregates on mechanical properties of concrete. Following paragraphs highlight previous works on examining the properties of recycled aggregate concrete (RAC) in comparison to natural aggregate concrete.

Research works on recycling of brick aggregates (B-waste) were initiated in 1990s [4–6]. Vrijders & Desmyter [7] suggested that the tendency of recycled aggregates to absorb more water than natural aggregates play a crucial role in determining mechanical properties of RAC. It was suggested that the mortar adhered to recycled aggregates increases their porosity resulting in 5–10 times higher water absorption than natural aggregates. Novakova & Mikulica [8] concluded that RAC exhibits five to fifteen times lower particle density as compared to natural aggregate concrete attributed to the lower density of surface adhered mortar in recycled aggregates. Debieb & Kenai [9] reported that the compressive strength of RAC reduced by 30% of that of the natural aggregate concrete when 100% of natural aggregates were replaced by recycled aggregates. Yang et al. [10] reported 11 and 20% reduction in concrete compressive strength when 20 and 50% natural aggregates were replaced by fired-clay brick aggregates. Medina et al. [11] found that compressive strength reduced up to 39% when 40% of natural aggregates were replaced by recycled aggregates. Cachim P [11] concluded that concrete properties were not affected by the replacement ratio up to 15%. For 30% replacement ratio, concrete properties were reduced up to 20%. González et al. [12] concluded that maximum reduction in compressive strength is 28%

when 100% of natural aggregates were replaced by recycled brick aggregates. Tensile strength of concrete was maintained up to the replacement ratio of 35%. A sharp decline in tensile strength was observed up to 30% of its initial strength at 100% replacement ratio. Authors suggested that lower resistance to fragmentation, lower density, and higher water absorption that natural aggregates are the catalysts for these inferior properties of recycled brick aggregate concrete. Jiang et al. [13] also concluded from monotonic axial compression tests on recycled brick aggregate concrete that an upper limit of 30% on the replacement ratio of natural aggregates (with recycled brick aggregates) must be imposed to sustain the strength and stiffness suitable for structural applications. Other works have also reported similar observations [14–16].

Literature presented in preceding paragraphs suggest that concrete produced from recycled brick aggregates exhibits inferior properties than those of natural aggregate concrete. However, the difference is minimal when the replacement ratio of natural aggregates by recycled brick aggregates is below 30%. Acknowledging this, current study aims to improve the substandard and inferior mechanical properties of recycled brick aggregate concrete for replacement ratios higher than 30%. A prevalent solution to improve substandard compressive strength of concrete fabricated with recycled brick aggregates can be practiced by wrapping it using different synthetic and natural fiber reinforced polymer (FRP) sheets. Although now-a-days, readily available synthetic FRPs are common in structural strengthening works [17–22] and improving structural properties of RAC [23–28], their expensive cost is a major concern [29–31]. Further, these FRPs are synthesized using chemicals that are capable of imparting skin issues such as irritant and allergic contact dermatitis for concerned personnel [32–34]. Recently, a possible solution was proposed to replace these synthetic fibers using natural fibers [35,36]. Salient features of natural FRPs include their substantial low costs in comparison to synthetic FRPs and do not carry risk to skin diseases as associated with synthetic FRPs [37–40]. There are several drawbacks of natural FRPs such as higher moisture absorption, inferior fire resistance, lower mechanical properties and durability. Many researchers have been working to address these issues, with particular attention paid to the surface treatment of fibers and improving the fiber/matrix interface.

In contrast to natural FRPs, Rousakis T.C. [41,42] proposed the use of ropes made of natural fibers as means of external confinement. Low-cost, easy availability, simple application, and environment friendly attributes of fiber ropes were emphasized. It was found that dry vinylon and polypropylene fibers were effective in improving ultimate strength and strain of concrete. Hussain et al. [43] investigated the effect of sisal, jute, and hemp fibers on ultimate compressive strength and corresponding strain of concrete. It was found that specimens confined with hemp fiber ropes exhibited highest gain in ultimate compressive strength. Fragoudakis et al. [44] examined the efficacy of hemp ropes to enhance bending strain and deflection of concrete beams and significant improvement in these parameters was reported. Ghalieh et al. [45] wrapped concrete columns with hemp ropes in three layers. Different slenderness ratios of columns were considered. Confined columns were found to demonstrate increased axial strength and ductility than their corresponding reference columns.

This study aims to improve the substandard mechanical properties of recycled aggregate concrete comprising brick aggregates (RAC-BA) replacing natural aggregates in excess of 30% replacement ratios. Low-cost, environmentally friendly, and easy-to-use hemp fiber ropes are chosen for this purpose. Research parameters included strength of concrete and the quantity of external hemp fibers (i.e., the number of hemp rope layers). Confinement efficacy of hemp fiber ropes on RAC-BA was assessed in terms of the gain in axial strength and ductility.

2. Experimental Program

2.1. Test Matrix

Sixteen concrete cylinders of standard size of 150 mm × 300 mm (diameter × height) were cast in this study in two batches. Eight cylinders were cast in each batch. Concrete

strength for the 1st and 2nd batches was 15 and 35 MPa, respectively. Depending upon the concrete strength, cylinders were grouped in groups A and B, respectively. For each group, two cylinders were tested in as-built condition i.e., serving as reference. Two cylinders each were strengthened with 1, 2, and 3 layers of hemp fiber ropes. Therefore, each group comprised 4 different cylinder configurations and two cylinders for each configuration type. The construction and strengthening cost is very high for these specimens at laboratory levels, therefore, in this study only 2 specimens were prepared and tested for each configuration. Table 1 presents details of the test matrix adopted in this study. Nomenclature of test specimens was chosen to represent their geometrical shape (“CIR” for circular), concrete strength (i.e., LSC and HSC for low and high strength, respectively), external strengthening configuration (i.e., CNT, 1HR, 2HR, and 3HR for the control, 1, 2, and 3 layers of hemp ropes, respectively) and specimen number in each configuration type (i.e., 01 and 02 for the two specimens tested in each configuration type).

Table 1. Details of test specimens.

Group	Specimen	Strength (MPa)	Layers of Hemp RFRP
A	CIR-LSC-CNT-01	Low strength concrete	-
	CIR-LSC-CNT-02	Low strength concrete	-
	CIR-LSC-1HR-01	Low strength concrete	1
	CIR-LSC-1HR-02	Low strength concrete	1
	CIR-LSC-2HR-01	Low strength concrete	2
	CIR-LSC-2HR-02	Low strength concrete	2
	CIR-LSC-3HR-01	Low strength concrete	3
	CIR-LSC-3HR-02	Low strength concrete	3
B	CIR-HSC-CNT-01	High strength concrete	-
	CIR-HSC-CNT-02	High strength concrete	-
	CIR-HSC-1HR-01	High strength concrete	1
	CIR-HSC-1HR-02	High strength concrete	1
	CIR-HSC-2HR-01	High strength concrete	2
	CIR-HSC-2HR-02	High strength concrete	2
	CIR-HSC-3HR-01	High strength concrete	3
	CIR-HSC-3HR-02	High strength concrete	3

2.2. Material Properties

Two concrete batches were used to cast 8 cylinders each corresponding to target strength of 15 and 35 MPa. Type-I Portland cement was used. Required amount of water was estimated to yield slumps of 90 and 70 mm for low and high strength concrete, respectively. Cement-clay interlocking bricks were used to replace natural coarse aggregates. For each concrete batch, 50% of natural aggregates were replaced with recycled brick aggregates. Figure 2a shows the cement-clay interlocking brick whereas Figure 2b presents brick crushing machine to yield aggregates with maximum size of 25 mm. The mechanical properties of bricks such as density, compressive strength and water absorption were found as per ASTM standards [46,47]. Density, compressive strength, and water absorption of the bricks were 145 (kg/m³), 6.26 (MPa), and 12.30%, respectively. Mix proportions of concrete are presented in Table 2.

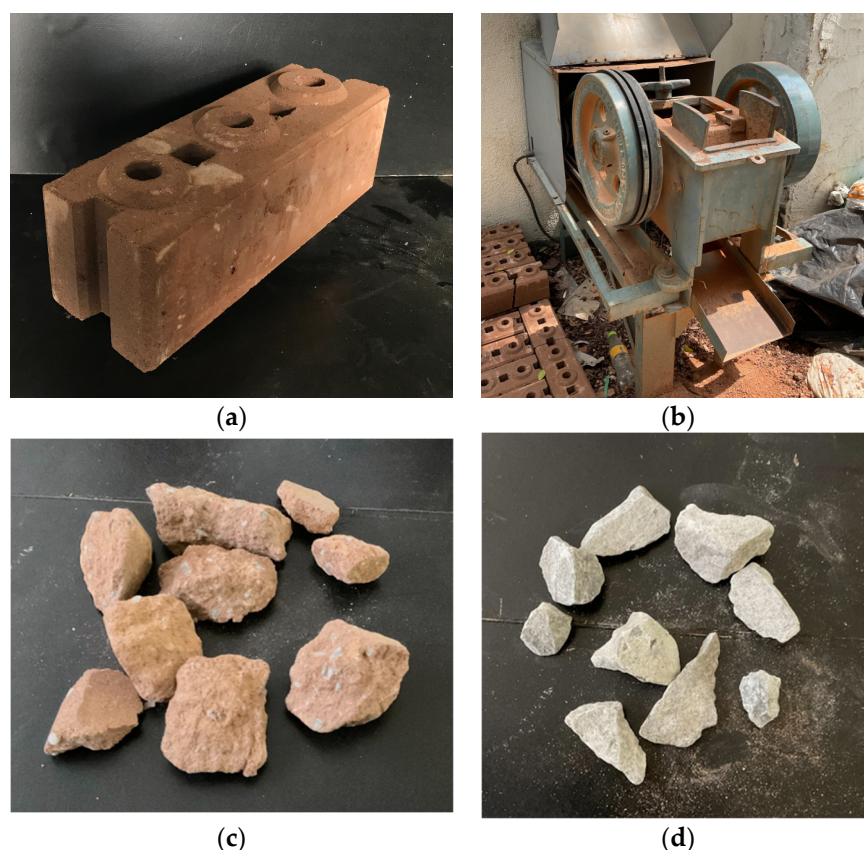


Figure 2. (a) Cement-clay interlocking brick (b) brick crushing machine (c) crushed brick aggregates and (d) natural stone aggregates.

Table 2. Mix proportions of concrete.

Mix Ingredients (kg/m ³)	Low Strength Concrete (15 MPa)	High Strength Concrete (35 MPa)
Cement	242	444
Fine aggregates	726	605
Natural coarse aggregates	605	504
Clay brick aggregates	605	504

A two-part epoxy was used to bond hemp ropes to specimen. Resin and hardener were mixed in 2:1. Resulting epoxy can easily be applied to bond hemp ropes and concrete surface using either a hand brush or roller. Physical properties of epoxy resin are given in Table 3. Tensile properties of hemp fiber ropes were determined in accordance with ASTM A931-18 [48] and ASTM E8/E8M-13 [49]. Sample ropes were tested under a displacement-controlled loading of 1.5 mm/min. Peak tensile stress was calculated from the nominal area of ropes. Nominal diameter of hemp ropes was 2.1 mm and its ultimate tensile stress was approximated as 137.4 MPa corresponding to a strain of 3.5%.

Table 3. Mechanical Properties of epoxy (as provided).

Property	Value
Ultimate Elongation (%)	2.5
Flexural Strength (MPa)	75
Tensile Strength (MPa)	50
Curing Time (hours)	6–10

2.3. Strengthening Process

Hemp fiber ropes were applied to concrete cylinders after 28 days of curing. Hussain et al. [43] found that inherent stress-strain response of hemp ropes constituted a flat plateau up to a stress of 10 MPa. This followed a slight transition into a steep stress-strain curve. Therefore, a pretension stress of 10 MPa was applied to the ropes during strengthening process. For this purpose, a special mechanical system was designed analogous to the one used by Hussain et al. [43]. At the start, a super glue was used to fix one end of the rope to concrete surface. Then the rope was carefully attached to the surface. Special care was practiced avoiding any gap between consecutive ropes around the circumference. Figure 3a shows the wrapping process of hemp rope. Once full height of the cylinder was wrapped with the rope, end of the rope was fixed to the surface using super glue. At this point, the two-part epoxy was applied as shown in Figure 3b. It was made sure that the ropes were impregnated with sufficient epoxy and that it penetrated well to the concrete surface. A break of at least 12 h was taken before the application of 2nd hemp rope layer. Similar procedure was followed to apply subsequent hemp rope layers. It is to be mentioned that hemp ropes were applied in the same direction as that of the underneath layers. A fully wrapped and epoxy dried cylinder is shown in Figure 3c.

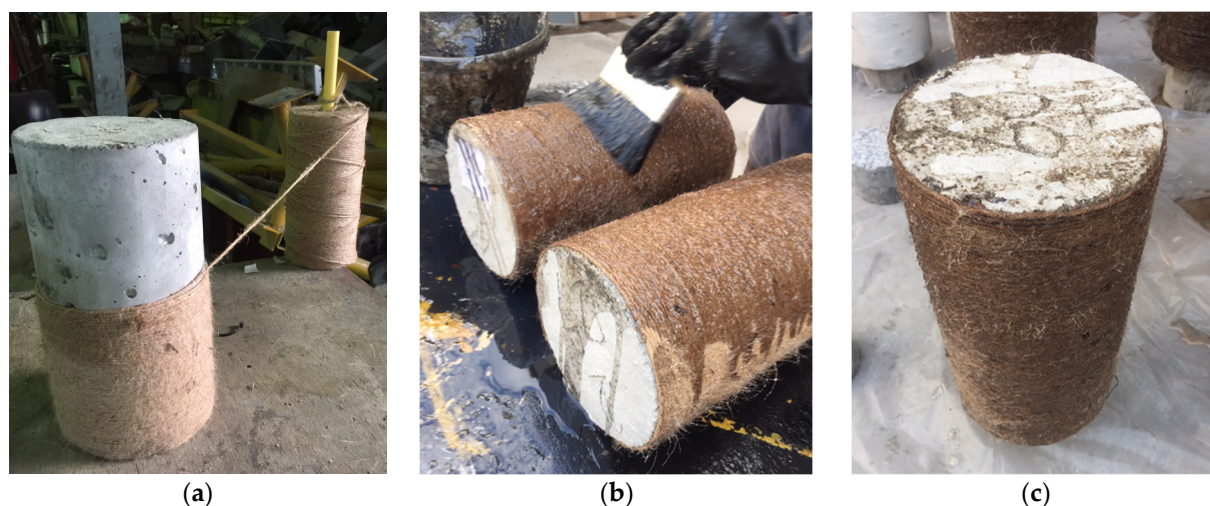


Figure 3. Strengthening process (a) application of hemp rope (b) epoxy impregnation in process and (c) fully wrapped and dried epoxy specimen.

2.4. Instrumentation & Loading Setup

Three Linear Variable Displacement Transducers (LVDTs) were applied around the circumference of specimens to record their axial deformations. A Universal Testing Machine (UTM) of 2MN capacity was used to apply monotonic compressive load on each specimen. Applied loading was displacement-controlled at a rate of 4000 N/s. To prevent accidental load transfer to the rope fiber shell at large axial deformations, two steel plates were attached to each cylinder's top and bottom side. Applied load intensity was monitored using a calibrated load cell placed at the top of specimen. Figure 4 presents typical test setup.

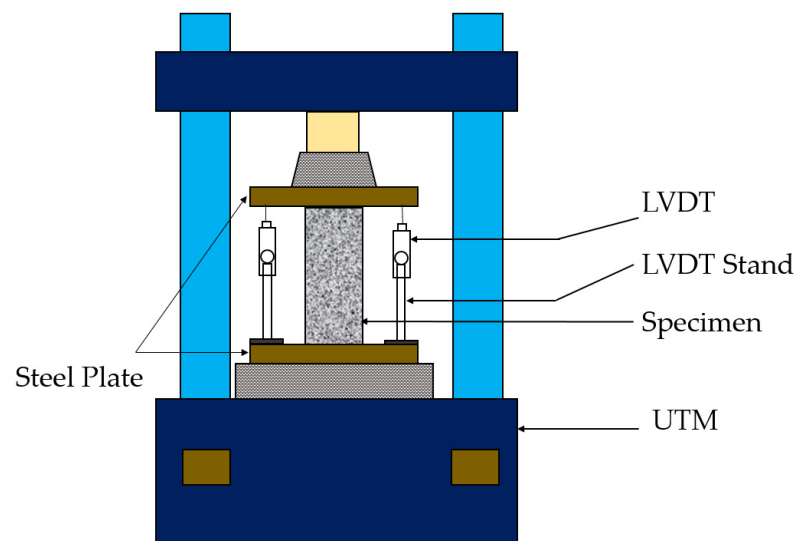


Figure 4. Test setup.

3. Experimental Results

3.1. Ultimate Failure Modes

Ultimate failure modes observed for each specimen type are shown in Figure 5. Failure of control cylinders accompanied crushing and splitting along the height of cylinders. More crushing was observed in high-strength control cylinder CIR-HSC-CNT as compared to that in low-strength cylinder CIR-LSC-CNT. Further, failure of high-strength control specimen was more explosive as compared to its counterpart low-strength specimen. Failure of all strengthened specimens occurred due to the tensile rupture of hemp ropes in hoop direction. No debonding of hemp ropes was observed indicating that the strength of epoxy was sufficient to bond hemp ropes and concrete surface throughout the load history without experiencing failure. For specimens strengthened with more than single layers of hemp ropes, snapping sounds were heard indicating progressive fracture of hemp ropes in underlying layers. Similar observations have been reported elsewhere [50,51]. For specimens confined with 1 and 2 layers, tensile fracture of hemp ropes was mainly concentrated within the middle zone. Whereas tensile fracture of hemp ropes in case of 3 layers was distributed over larger area and propagated along the full height of cylinders. This observation has also been reported in previous research works [43,52].



Figure 5. Cont.



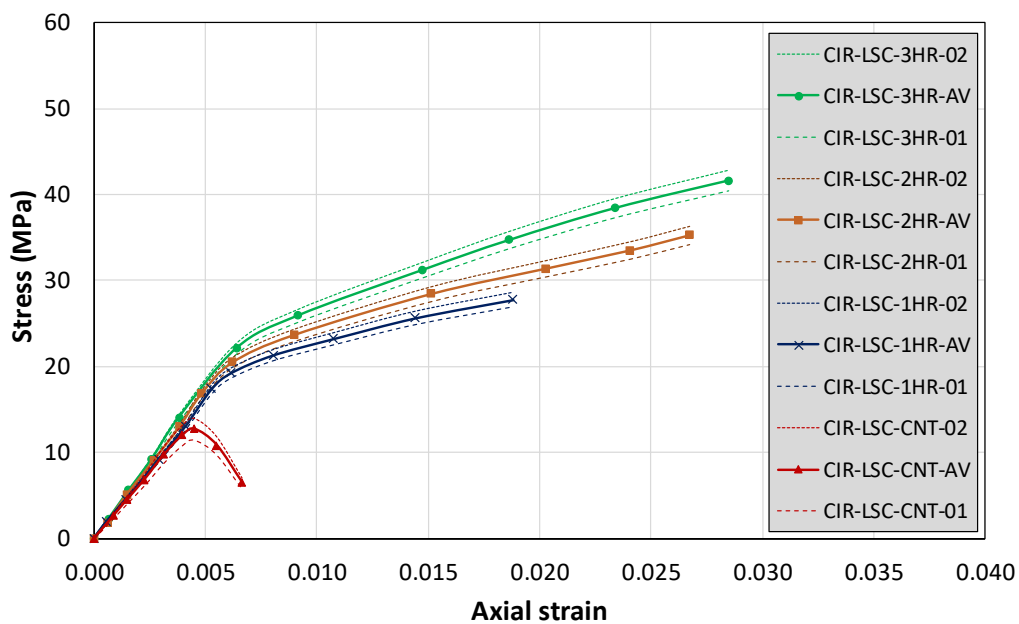
Figure 5. Ultimate failure modes.

3.2. Axial Stress-Strain Response

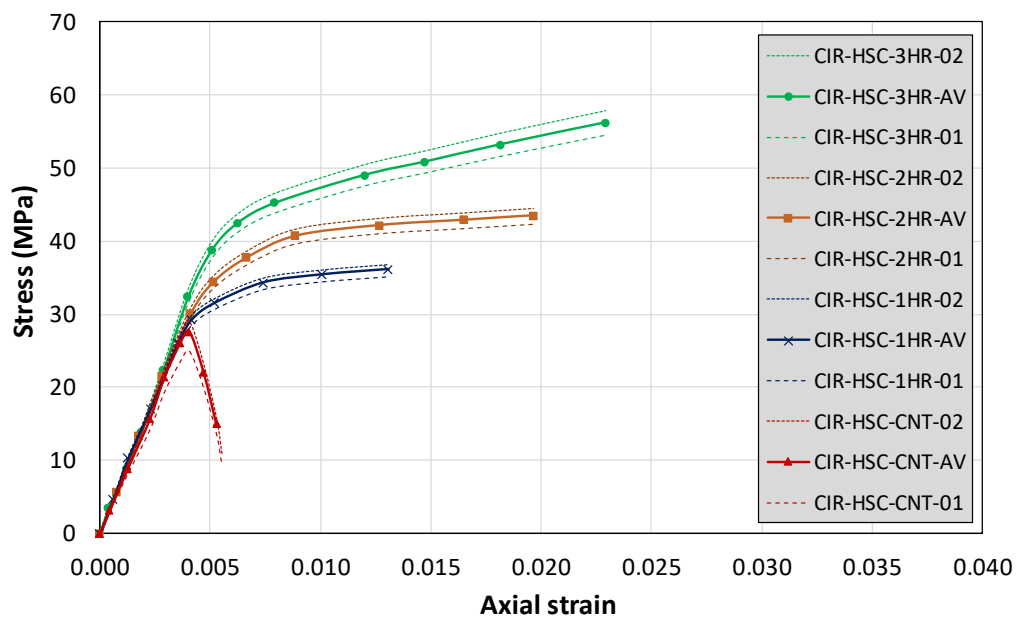
Table 2 provides summary of experimental results in terms of ultimate axial strength, corresponding strain, increase in ultimate strength, and corresponding strain for all specimens. The results are reported in Figure 6 for each specimen along with the average results. During the test, the data was collected for a specific load intervals and average was calculated by adding up stress and axial strain data, then dividing the total by the count of numbers. It is evident that control specimens in both groups experienced brittle failure at their peak compressive loads recognized by sudden drop in their axial carrying capacities. Whereas all strengthened specimens demonstrated a bilinear axial stress-strain response. From Figure 6, it is also shown that ultimate strength and corresponding strain increased as the number of hemp rope layers increased. However, the onset of second branch of axial stress-strain of strengthened specimens occurred at similar axial strain levels. Further, initial slope of all specimens could not be differentiated. From Table 4, for group A specimens, increase in ultimate strength over that of control specimen was 83, 157, and 209% for 1-, 2-, and 3-layer confinement of hemp ropes. Similarly, strain at ultimate strength increased by 321, 477, and 539% for 1-, 2-, and 3-layer confinement. A similar trend in the increase in ultimate strength and corresponding strain was observed for group B specimens. It can be established that hemp ropes were able to impart substantial ductility to the concrete irrespective of the number of their layers.

Table 4. Summary of experimental results.

Group	Specimen	Ultimate Stress (MPa)	Increase in Ultimate Stress (%)	Ultimate Strain	Increase in Ultimate Strain (%)
A	CIR-LSC-CNT	13.02	-	0.0044	-
	CIR-LSC-1HR	23.77	83	0.0187	321
	CIR-LSC-2HR	33.39	157	0.0256	477
	CIR-LSC-3HR	40.18	209	0.0283	539
B	CIR-HSC-CNT	24.34	-	0.0041	-
	CIR-HSC-1HR	36.22	49	0.0132	219
	CIR-HSC-2HR	43.58	79	0.0193	368
	CIR-HSC-3HR	56.03	130	0.0229	454



(a)



(b)

Figure 6. Axial stress-strain response of cylinders in (a) group A and (b) group B.

3.3. Effect of Hemp Rope Layers & Concrete Strength

Figure 7 presents increase in ultimate compressive strength and corresponding strain of hemp rope confined specimens. It can be seen that the increase in ultimate strength and corresponding strain in low-strength concrete specimens was higher as compared to the increase in high-strength concrete specimens for same amount of hemp rope confinements. For ultimate strength, low-strength concrete specimens experienced up to 79% higher increase as compared to high-strength concrete specimens. Similarly, up to 109% higher increase ultimate strain was observed for low-strength concrete specimens for similar amount of hemp confinement. Nonetheless, a positive correlation is observed in the

increase in ultimate strength and strain with the number of hemp rope layers. This trend existed irrespective of the type of constituting concrete i.e., low or high strength.

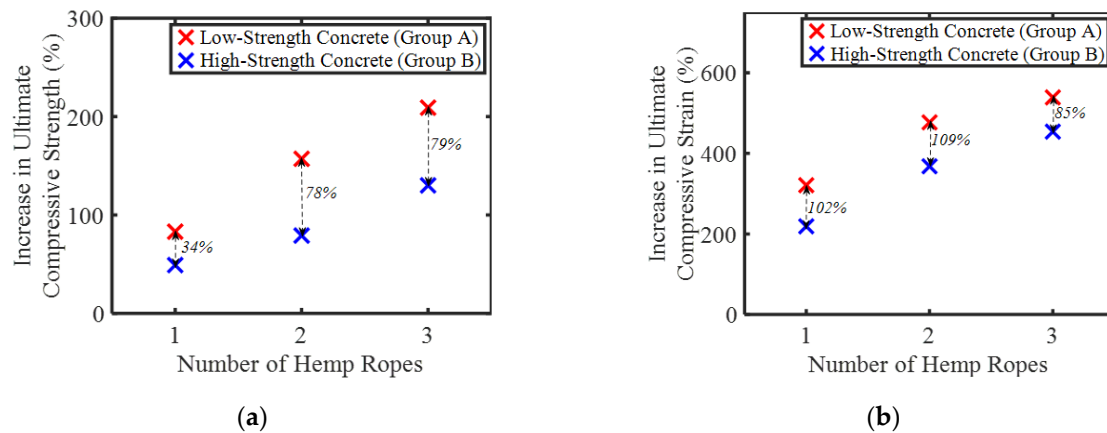


Figure 7. Increase in ultimate compressive (a) strength and (b) corresponding strain.

3.4. Analytical Investigations

3.4.1. Peak Axial Strength Models

Numerous equations in literature exist that relate to axial strength enhancement of concrete due to the externally wrapped FRPs [53,54]. The confined peak strength is often stated in the following form:

$$\frac{f_{ch}}{f'_c} = 1 + k_1 \frac{f_l}{f'_{co}} \quad (1)$$

where f_{ch} represents peak compressive strength due to hemp rope confinement, k_1 is a constant that varies in different models and f_l is the passive pressure applied by external wraps. It can be approximated by establishing equilibrium between outward bursting pressure and resulting confining stresses in external wraps in hoop direction as shown in Figure 8 and given in Equation (2).

$$f_l = \frac{2f_t t}{D} \quad (2)$$

where f_t and D are tensile strength of external wraps and diameter of the specimen, respectively. For hemp confined concrete, ultimate tensile strength of hemp rope is used whereas thickness " t " corresponds to the nominal diameter of a single hemp rope. Confining pressure on cylinders confined with more than single hemp fiber ropes was estimated by multiplying Equation (2) by the number of hemp fiber ropes. Several existing peak axial strength models are given in Table 5.

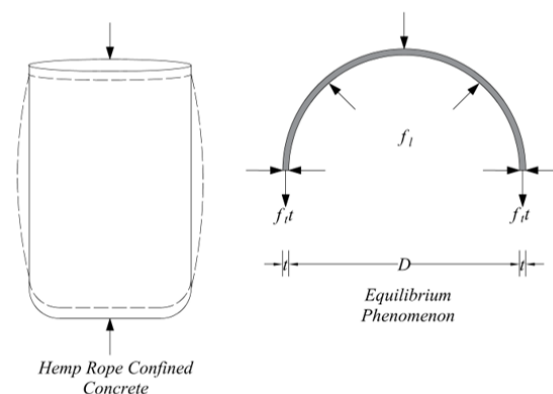


Figure 8. Hemp confined concrete and resulting equilibrium forces under compression.

3.4.2. Peak Axial Strain Models

One of the initial studies on lateral confining on concrete was presented by Richart et al. [55]. Ultimate axial strain can be related to externally applied pressure f_l using Equation (3).

$$\frac{\epsilon_{cc}}{\epsilon_{co}} = 1 + k_2 \frac{f_l}{f_{co}} \quad (3)$$

where ϵ_{co} is the axial peak strain of unconfined concrete. Richart et al. [55] proposed a value of $5k_1$ for k_2 in the case of steel confined concrete. It has been established that the same form of Equation (2) can be extended to FRP confined concrete [53,56–58]. In this study, existing ultimate strain models are assessed by assuming that hemp fiber ropes provide confinement in a similar manner as other FRP confinement systems. Table 5 presents several ultimate stress and strain models for externally confined cylinders.

Table 5. Existing stress-strain models.

ID	Model	Expression for Peak Stress f'_{cc}	Expression for Peak Strain ϵ'_{cc}
1	Richart et al. [55]	$\frac{f'_{cc}}{f'_{co}} = 1 + 4.10 \frac{f_l}{f'_{co}}$	$\frac{\epsilon'_{cc}}{\epsilon_o} = 1 + 5 \left(\frac{f'_{cc}}{f'_{co}} - 1 \right)$
2	Ghernouti and Rabehi [59]	$\frac{f'_{cc}}{f'_{co}} = 1 + 2.038 \frac{f_l}{f'_{co}}$	$\frac{\epsilon'_{cc}}{\epsilon_o} = 1 + 10.56 \left(\frac{f_l}{f_o} \right)$
3	Benzaid et al. [60]	$\frac{f'_{cc}}{f'_{co}} = 1 + 2.20 \frac{f_l}{f'_{co}}$	$\frac{\epsilon'_{cc}}{\epsilon_o} = 2 + 7.6 \left(\frac{f_l}{f_o} \right)$
4	Al-Salloum [61]	$\frac{f'_{cc}}{f'_{co}} = 1 + 2.312 \frac{f_l}{f'_{co}}$	$\frac{\epsilon'_{cc}}{\epsilon_o} = 1 + 0.024 \left(\frac{f_l}{f_o} \right)$
5	Bisby et al. [62]	$\frac{f'_{cc}}{f'_{co}} = 1 + 2.425 \frac{f_l}{f'_{co}}$	-
6	Wu et al. [63]	$\frac{f'_{cc}}{f'_{co}} = 1 + 3.20 \frac{f_l}{f'_{co}}$	$\frac{\epsilon'_{cc}}{\epsilon_o} = 1 + 9.5 \left(\frac{f_l}{f_o} \right)$
7	Teng et al. [64]	$\frac{f'_{cc}}{f'_{co}} = 1 + 3.50 \frac{f_l}{f'_{co}}$	$\frac{\epsilon'_{cc}}{\epsilon_o} = 1 + 17.5 \left(\frac{f_l}{f_o} \right)^{1.2}$
8	Ahmad and Shah [65]	$\frac{f'_{cc}}{f'_{co}} = 1 + 4.2556 \frac{f_l}{f'_{co}}$	-
9	Hussain et al. [66]	$\frac{f'_{cc}}{f'_{co}} = 1 + 6.40 \frac{f_l}{f'_{co}}$	-
10	Karbhari and Gao [67]	$\frac{f'_{cc}}{f'_{co}} = 1 + 2.1 \left(\frac{f_l}{f'_{co}} \right)^{0.87}$	-
11	Samaan et al. [68]	$\frac{f'_{cc}}{f'_{co}} = 1 + 6.0 \frac{f_l^{0.70}}{f'_{co}}$	-
12	Miyauchi et al. [56]	$\frac{f'_{cc}}{f'_{co}} = 1 + 3.50 \frac{f_l}{f'_{co}}$	$\frac{\epsilon'_{cc}}{\epsilon_o} = 1 + 10.6 \left(\frac{f_l}{f_o} \right)^{0.373}$
13	Saafi et al. [69]	$\frac{f'_{cc}}{f'_{co}} = 1 + 2.20 \left(\frac{f_l}{f'_{co}} \right)^{0.84}$	-
14	Ilki and Kumbasar [70]	$\frac{f'_{cc}}{f'_{co}} = 1 + 2.227 \frac{f_l}{f'_{co}}$	$\frac{\epsilon'_{cc}}{\epsilon_o} = 1 + 15.15 \left(\frac{f_l}{f_o} \right)^{0.735}$
15	Spoelstra and Monti [71]	$\frac{f'_{cc}}{f'_{co}} = 0.2 + 3 \left(\frac{f_l}{f'_{co}} \right)^{0.50}$	$\frac{\epsilon'_{cc}}{\epsilon_o} = 1 + 1.25 \left(\frac{f_l}{f_o} \right)^{0.5}$
16	Mirmiran [72]	-	-
17	Pimanmas et al. [73]	$\frac{f'_{cc}}{f'_{co}} = 1 + 3.0 \frac{f_l}{f'_{co}}$	$\frac{\epsilon'_{cc}}{\epsilon_o} = 2 + 6.7 \left(\frac{f_l}{f_o} \right)$
18	Yan [74]	$\frac{f'_{cc}}{f'_{co}} = 1 + 1.86 \frac{f_l}{f'_{co}}$	-
19	Hussain et al. [43]	$\frac{f'_{cc}}{f'_{co}} = 1 + 2.7 \frac{f_l}{f'_{co}}$	$\frac{\epsilon'_{cc}}{\epsilon_o} = 2 + 10 \left(\frac{f_l}{f_o} \right)$

Figure 9 presents the comparison between analytically predicted peak axial strengths and corresponding strains. For clarity, the comparison is plotted for each specimen type separately. Figure 9a presents the comparison of analytical and experimental peak axial strengths for group A specimens. It is noticed that several analytical models were able to predict experimental axial strength with good accuracy. However, the models of

Wu et al. [63], Teng et al. [64], Richart et al. [55], Ahmad and Shah [65], Hussain et al. [66] significantly overestimated axial strengths. Same models also overestimated peak axial strengths of group B specimens. Remaining models demonstrated close agreement with experimental values and other statistical indicators were required to quantify their accuracy.

In general, most of the existing ultimate strain models overestimated experimental ultimate axial strains for group A specimens (see Figure 9c). For three specimens in group A, the model of Pimanmas et al. was able to provide close agreement with experimental results. Ultimate axial strain for group B specimens was closely predicted by the models of Ghernouti and Rabehi [59], Benzaid et al. [60], Pimanmas et al. [73], and Hussain et al. [43]. The model of Hussain et al. was proposed for hemp rope confinement on natural aggregate concrete. It is interesting to note that this model predicted experimental peak axial strains for high strength concrete recycled aggregate concrete specimens only.

Statistical indicators of average absolute error ($AAR\%$) and average ratio (AR) were used to assess the performance of considered analytical models in this study. AAR provides an estimate of the average of absolute value of the difference between experimental and analytical value. AR provides an average value that quantifies the extent of over-/underestimation of the predicted value in comparison to the corresponding experimental result. An AR value greater than 1 means overestimation whereas underestimation is related to an AR value smaller than 1. AAR and AR are calculated using Equations (4) and (5), respectively [75].

$$AAR = \frac{\sum_{i=1}^N \left| \frac{\text{Theoretical} - \text{Experimental}}{\text{Theoretical}} \right|}{N} \quad (4)$$

$$AR = \frac{\sum_{i=1}^N \frac{\text{Theoretical}}{\text{Experimental}}}{N} \quad (5)$$

where N is the total number of observations. Table 6 provides calculated AAR and AR values for all analytical models. Last two rows of Table 6 summarize those models that resulted in AAR and AR less than 10% and $0.90 \leq AR \leq 1.10$, respectively. For ultimate strength of group A specimens (i.e., low strength concrete), the models of Benzaid et al. [60], Al-Salloum [61], Bisby et al. [62], Karbhari and Gao [67], Saafi et al. [69], Saafi et al. [69], Spoelstra and Monti [71], and Hussain et al. [43] provided results within considered thresholds. In addition to these models, the models of Wu et al. [63], Samaan et al. [68], and Pimanmas et al. [73] also resulted in analytical values within thresholds for group B specimens. Interestingly, none of the considered models resulted AAR value less than 10% for peak strain of group A specimens. Whereas the model of Pimanmas et al. [73] was found to be the only model resulting in AR value between 0.9 and 1.1 for the same group. For group B specimens, the models of Ghernouti and Rabehi [59], Benzaid et al. [60], and Pimanmas et al. [73] provided analytical peak strains with reasonable accuracy.

It can be established that the model of Benzaid et al. [60] and Pimanmas et al. [73] were standout among other models and consistently predicted experimental peak axial strengths and strains with reasonable accuracy. Further, it can also be noted that the performance of existing models was better in predicting experimental peak strengths than their tendency to predict experimental peak axial strains. Another observation can be made regarding the strength of inherent concrete. For low-strength concrete specimens, performance of existing models was found inferior that that for high-strength concrete.

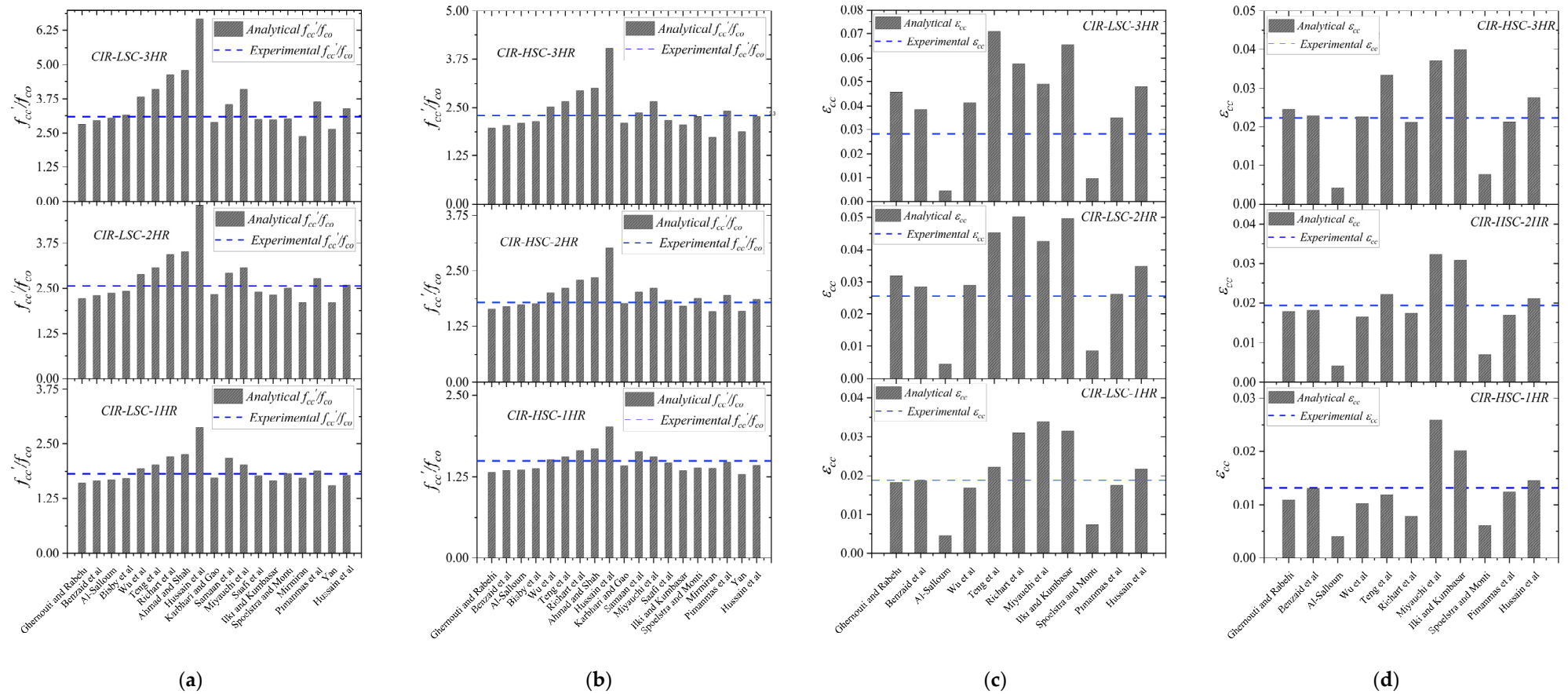


Figure 9. Comparison of analytical versus experimental (a) peak strengths in group A (b) peak strengths in group B (c) peak strain in group A and (d) peak strain in group B.

Table 6. Summary of statistical indicators for each model.

Model	Ultimate Compressive Stress f'_{cc}				Ultimate Compressive Strain ϵ'_{cc}			
	Group #1		Group #2		Group #1		Group #2	
	AAR (%)	AR	AAR (%)	AR	AAR (%)	AR	AAR (%)	AR
Richart et al. [55]	34.93	0.90	22.30	0.75	88.66	2.83	18.54	1.88
Ghernouti and Rabehi [59]	11.78	0.88	11.30	0.89	29.53	1.27	11.81	0.95
Benzaid et al. [60]	8.11	0.92	8.66	0.91	15.84	1.16	3.37	0.98
Al-Salloum [61]	5.58	0.94	6.83	0.93	81.00	0.19	76.27	0.24
Bisby et al. [62]	4.39	0.97	6.83	0.95	-	-	-	-
Wu et al. [63]	14.55	1.14	7.63	1.07	23.53	1.17	12.84	0.88
Teng et al. [64]	21.34	1.21	12.52	1.12	82.35	1.83	24.66	1.18
Ahmad and Shah [65]	38.45	1.38	24.83	1.24	-	-	-	-
Hussain et al. [66]	87.03	1.87	59.77	1.59	-	-	-	-
Karbhari and Gao [67]	6.97	0.93	4.81	0.95	-	-	-	-
Samaan et al. [68]	16.23	1.16	8.60	1.08	-	-	-	-
Miyauchi et al. [56]	21.34	1.21	12.52	1.12	73.95	1.74	76.77	1.77
Saafi et al. [69]	3.66	0.96	3.15	0.98	-	-	-	-
Ilki and Kumbasar [70]	7.50	0.92	8.22	0.92	98.09	1.98	63.68	1.64
Spoelstra and Monti [71]	1.51	0.99	4.45	0.99	64.31	0.36	61.03	0.39
Mirmiran [72]	15.73	0.84	14.35	0.86	-	-	-	-
Pimanmas et al. [73]	10.01	1.10	4.99	1.04	10.74	1.06	7.42	0.93
Yan [74]	15.81	0.84	14.35	0.86	-	-	-	-
Hussain et al. [43]	4.23	1.03	2.86	0.99	40.48	1.40	14.95	1.15
$AAR (\%) \leq 10$	[41,58–60,65,67–69]		[41,58–61,65–69,71]		N/A		[58,71]	
$0.90 \leq AR \leq 10$	[41,58–60,65,67–69]		[41,58–61,65–69,71]		[71]		[57,58,71]	

4. Discussion

Natural fibers in the form of hemp ropes used in this study have shown their potential to enhance axial compressive strength of the concrete made with recycled brick coarse aggregate. Though the application of hemp ropes in this study was limited to cylindrical specimens, their application by no means is limited to small scale specimens. An existing study [36] has already extended the use of natural fibers to full scale shear deficient RC columns. It was found that the columns strengthened with natural fibers demonstrated similar improvement in shear strength as that of the columns strengthened with CFRP wraps.

5. Conclusions

Each year, massive amount of construction waste is generated that needs proper attention in terms of its disposal without deteriorating surrounding environment. A significant portion of this waste comprises bricks. Besides, large number of new constructions works resulting in the depletion of natural resources rapidly. Intuitively, a sustainable solution demands to reuse the construction waste in the best way possible. This study targeted brick waste as a potential material to be used as a partial replacement of natural aggregates in structural concrete. It has been known that concrete constructed with recycled brick aggregates possess substandard mechanical properties. Traditionally, synthetic FRPs are known to strengthen recycled aggregate concrete. However, recognizing high costs associated with them, this study proposed the use of natural hemp fiber ropes to strengthen RAC constructed with brick aggregates. To assess the efficacy of hemp ropes in strengthen-

ing mechanical properties of the concrete with coarse aggregates partially replaced with recycled brick aggregates, an experimental framework was conducted. Sixteen cylindrical specimens were tested in two groups depending upon the strength of concrete. Within each group, 2 specimens each were strengthened with 1, 2, and 3 layers of hemp fiber ropes. Axial monotonic compressive loading was applied to each specimen. Resulting axial stress-strain curves were compared with those of the reference specimens. Following important conclusions can be drawn.

1. Reference specimens exhibited typical concrete failure under compression. Negligible axial ductility was observed in stress-strain response.
2. For specimens strengthened with hemp fiber rope specimens, a bilinear axial stress-strain response was observed. This bilinear hardening behavior persisted irrespective of the number of external hemp rope layers resulting in significant improvement of axial ductility over that of the control specimens. By increasing the number of hemp rope layers, both peak axial strength and corresponding strain increased. Further, irrespective of the concrete strength, maximum peak compressive strength and strain were noticed for the case of 3-layer hemp rope confinement. Failure of hemp rope strengthened specimens was characterized by tensile rupture of hemp ropes in hoop direction. However, this was not before imparting significant ductility to the bare concrete.
3. Concrete strengths of 15 and 35 MPa were considered in this study. The performance of hemp ropes in improving peak strength and corresponding strain was found superior in low-strength concrete specimens for the same configurations of hemp ropes.
4. For the sake of performance-based non-linear modelling, accurate modelling at material level is necessary. For this purpose, several existing analytical stress-strain models were tested in this study to predict ultimate confined compressive strength and strain. It was found that a number of models predicted confined compressive strengths with reasonable accuracy. However, very few models were able to predict confined peak strain with good accuracy. It was established that the model of Benzaid et al. [60] and Pimanmas et al. [73] were standouts among other models and consistently predicted experimental peak axial strengths and strains with reasonable accuracy.
5. Future studies are required to further enhance the data base and to develop more accurate strength models by considering more approximate number of specimens and number of strengthening layers.

Author Contributions: Conceptualization, E.Y. and P.J.; Data curation, Q.H.; Methodology, P.J. and Q.H.; Investigation, E.Y. and A.R.; Formal analysis, P.J.; Funding acquisition, E.Y. and A.R.; Supervision, N.A.; Writing—original draft, P.J., K.C. and Q.H.; Writing—review & editing, E.Y., P.J., N.A. and K.C. All authors have read and agreed to the published version of the manuscript.

Funding: This research was funded by the Department of Civil Engineering, King Mongkut's University of Technology Thonburi (KMUTT) under Research Grant No. CE-KMUTT 6501.

Acknowledgments: This research was funded by the Department of Civil Engineering, King Mongkut's University of Technology Thonburi (KMUTT) under Research Grant No. CE-KMUTT 6501. The authors also like to extend their gratitude to the Asian Institute of Technology (AIT) for supporting test facilities.

Conflicts of Interest: The authors declare no conflict of interest.

References

1. Zheng, C.; Lou, C.; Du, G.; Li, X.; Liu, Z.; Li, L. Mechanical Properties of Recycled Concrete with Demolished Waste Concrete Aggregate and Clay Brick Aggregate. *Results Phys.* **2018**, *9*, 1317–1322. [[CrossRef](#)]
2. Zhu, L.; Zhu, Z. Reuse of Clay Brick Waste in Mortar and Concrete. *Adv. Mater. Sci. Eng.* **2020**, *2020*, 6326178. [[CrossRef](#)]
3. Manfredi, S.; Pant, R.; Pennington, D.W.; Versmann, A. Supporting Environmentally Sound Decisions for Waste Management with LCT and LCA. *Int. J. Life Cycle Assess.* **2011**, *16*, 937–939. [[CrossRef](#)]
4. Mansur, M.A.; Wee, T.H.; Cheran, L.S. Crushed Bricks as Coarse Aggregate for Concrete. *Mater. J.* **1999**, *96*, 478–484. [[CrossRef](#)]

5. Khalaf, F.M. Using Crushed Clay Brick as Coarse Aggregate in Concrete. *J. Mater. Civ. Eng.* **2006**, *18*, 518–526. [[CrossRef](#)]
6. Khalaf, F.M.; DeVenny, A.S. Recycling of Demolished Masonry Rubble as Coarse Aggregate in Concrete: Review. *J. Mater. Civ. Eng.* **2004**, *16*, 331–340. [[CrossRef](#)]
7. Vrijders, J.; Desmyter, J. Een Hoogwaardig Gebruik van Puinggranulaten Stimuleren. *OVAM Mechelen* **2008**.
8. Nováková, I.; Mikulica, K. Properties of Concrete with Partial Replacement of Natural Aggregate by Recycled Concrete Aggregates from Precast Production. *Procedia Eng.* **2016**, *151*, 360–367. [[CrossRef](#)]
9. Debieb, F.; Kenai, S. The Use of Coarse and Fine Crushed Bricks as Aggregate in Concrete. *Constr. Build. Mater.* **2008**, *22*, 886–893. [[CrossRef](#)]
10. Yang, J.; Du, Q.; Bao, Y. Concrete with Recycled Concrete Aggregate and Crushed Clay Bricks. *Constr. Build. Mater.* **2011**, *25*, 1935–1945. [[CrossRef](#)]
11. Medina, C.; Zhu, W.; Howind, T.; Sánchez De Rojas, M.I.; Frías, M. Influence of Mixed Recycled Aggregate on the Physical—Mechanical Properties of Recycled Concrete. *J. Clean. Prod.* **2014**, *68*, 216–225. [[CrossRef](#)]
12. González, J.S.; Gayarre, F.L.; Pérez, C.L.C.; Ros, P.S.; López, M.A.S. Influence of Recycled Brick Aggregates on Properties of Structural Concrete for Manufacturing Precast Prestressed Beams. *Constr. Build. Mater.* **2017**, *149*, 507–514. [[CrossRef](#)]
13. Jiang, T.; Wang, X.M.; Zhang, W.P.; Chen, G.M.; Lin, Z.H. Behavior of FRP-Confined Recycled Brick Aggregate Concrete under Monotonic Compression. *J. Compos. Constr.* **2020**, *24*, 04020067. [[CrossRef](#)]
14. Kou, S.C.; Poon, C.S.; Chan, D. Influence of Fly Ash as Cement Replacement on the Properties of Recycled Aggregate Concrete. *J. Mater. Civ. Eng.* **2007**, *19*, 709–717. [[CrossRef](#)]
15. Jin, C.; Wang, X.; Akinkulore, O.O.; Jiang, C.R. Experimental Research on the Conversion Relationships. *Chin. Concr. J.* **2008**, *11*, 37–39.
16. Jiabin, L.; Jianzhuang, X.; Jian, H. Influence of Recycled Coarse Aggregate Replacement Percentages on Compressive Strength of Concrete. *Jianzhu Cailiao Xuebao/J. Build. Mater.* **2006**, *9*, 297–301.
17. Ameli, M.; Ronagh, H.R.; Dux, P.F. Behavior of FRP Strengthened Reinforced Concrete Beams under Torsion. *J. Compos. Constr.* **2007**, *11*, 192–200. [[CrossRef](#)]
18. Attari, N.; Amziane, S.; Chemrouk, M. Flexural Strengthening of Concrete Beams Using CFRP, GFRP and Hybrid FRP Sheets. *Constr. Build. Mater.* **2012**, *37*, 746–757. [[CrossRef](#)]
19. Antonopoulos, C.P.; Triantafyllou, T.C. Experimental Investigation of FRP-Strengthened RC Beam-Column Joints. *J. Compos. Constr.* **2003**, *7*, 39–49. [[CrossRef](#)]
20. Smith, S.T.; Hu, S.; Kim, S.J.; Seracino, R. FRP-Strengthened RC Slabs Anchored with FRP Anchors. *Eng. Struct.* **2011**, *33*, 1075–1087. [[CrossRef](#)]
21. Smith, S.T.; Teng, J.G. FRP-Strengthened RC Beams. I: Review of Debonding Strength Models. *Eng. Struct.* **2002**, *24*, 385–395. [[CrossRef](#)]
22. Belarbi, A.; Acun, B. FRP Systems in Shear Strengthening of Reinforced Concrete Structures. *Procedia Eng.* **2013**, *57*, 2–8. [[CrossRef](#)]
23. Jiangfeng, D.; Shucheng, Y.; Qingyuan, W.; Wenyu, Z.; Jiangfeng, D.; Shucheng, Y.; Qingyuan, W.; Wenyu, Z. Flexural Behavior of RC Beams Made with Recycled Aggregate Concrete and Strengthened by CFRP Sheets. *J. Build. Struct.* **2019**, *40*, 71–78. [[CrossRef](#)]
24. Liang, J.; Lin, S.; Ahmed, M. Axial Behavior of Carbon Fiber-Reinforced Polymer-Confined Recycled Aggregate Concrete-Filled Steel Tube Slender Square Columns. *Adv. Struct. Eng.* **2021**, *24*, 3507–3518. [[CrossRef](#)]
25. Chen, G.M.; Zhang, J.J.; Jiang, T.; Lin, C.J.; He, Y.H. Compressive Behavior of CFRP-Confined Recycled Aggregate Concrete in Different-Sized Circular Sections. *J. Compos. Constr.* **2018**, *22*, 04018021. [[CrossRef](#)]
26. Li, P.; Zhao, Y.; Long, X.; Zhou, Y.; Chen, Z. Ductility Evaluation of Damaged Recycled Aggregate Concrete Columns Repaired With Carbon Fiber-Reinforced Polymer and Large Rupture Strain FRP. *Front. Mater.* **2020**, *7*, 346. [[CrossRef](#)]
27. Khan, A.R.; Fareed, S.; Nasir, R.; Xiao, J. Behaviour and Strength Prediction of Reinforced Recycled Aggregate Concrete Columns Confined with CFRP Wraps. *Iran. J. Sci. Technol. Trans. Civ. Eng.* **2021**, 1–13. [[CrossRef](#)]
28. Chen, G.M.; He, Y.H.; Jiang, T.; Lin, C.J. Behavior of CFRP-Confined Recycled Aggregate Concrete under Axial Compression. *Constr. Build. Mater.* **2016**, *111*, 85–97. [[CrossRef](#)]
29. Iskander, M.G.; Hassan, M. State of the Practice Review in FRP Composite Piling. *J. Compos. Constr.* **1998**, *2*, 116–120. [[CrossRef](#)]
30. Wang, X.; Wu, Z. Evaluation of FRP and Hybrid FRP Cables for Super Long-Span Cable-Stayed Bridges. *Compos. Struct.* **2010**, *92*, 2582–2590. [[CrossRef](#)]
31. Chaiyasarn, K.; Hussain, Q.; Joyklad, P.; Rodsin, K. New Hybrid Basalt/E-Glass FRP Jacketing for Enhanced Confinement of Recycled Aggregate Concrete with Clay Brick Aggregate. *Case Stud. Constr. Mater.* **2021**, *14*, e00507. [[CrossRef](#)]
32. Tarvainen, K.; Jolanki, R.; Forsman-Grönholm, L.; Estlander, T.; Pfäffli, P.; Juntunen, J.; Kanerva, L. Exposure, Skin Protection and Occupational Skin Diseases in the Glass-Fibre-Reinforced Plastics Industry. *Contact Dermat.* **1993**, *29*, 119–127. [[CrossRef](#)]
33. Tarvainen, K.; Jolanki, R.; Estlander, T. Occupational Contact Allergy to Unsaturated Polyester Resin Cements. *Contact Dermat.* **1993**, *28*, 220–224. [[CrossRef](#)] [[PubMed](#)]
34. Minamoto, K.; Nagano, M.; Inaoka, T.; Kitano, T.; Ushijima, K.; Fukuda, Y.; Futatsuka, M. Skin Problems among Fiber-Glass Reinforced Plastics Factory Workers in Japan. *Ind. Health* **2002**, *40*, 42–50. [[CrossRef](#)]
35. Yin, S.; Hussain, Q.; Joyklad, P.; Chaimahawan, P.; Rattanapitikon, W.; Limkatanyu, S.; Pimanmas, A. Strengthening Effect of Natural Fiber Reinforced Polymer Composites (NFRP) on Concrete. *Case Stud. Constr. Mater.* **2021**, *15*, e00653. [[CrossRef](#)]

36. Yooprasertchai, E.; Wiwatrojanagul, P.; Pimanmas, A. A Use of Natural Sisal and Jute Fiber Composites for Seismic Retrofitting of Nonductile Rectangular Reinforced Concrete Columns. *J. Build. Eng.* **2022**, *52*, 104521. [[CrossRef](#)]
37. Jirawattanasomkul, T.; Likitlersuang, S.; Wuttiwannasak, N.; Ueda, T.; Zhang, D.; Shono, M. Structural Behaviour of Pre-Damaged Reinforced Concrete Beams Strengthened with Natural Fibre Reinforced Polymer Composites. *Compos. Struct.* **2020**, *244*, 112309. [[CrossRef](#)]
38. Sen, T.; Jagannatha Reddy, H.N. Efficacy of Bio Derived Jute FRP Composite Based Technique for Shear Strength Retrofitting of Reinforced Concrete Beams and Its Comparative Analysis with Carbon and Glass FRP Shear Retrofitting Schemes. *Sustain. Cities Soc.* **2014**, *13*, 105–124. [[CrossRef](#)]
39. Li, Y.; Mai, Y.W.; Ye, L. Sisal Fibre and Its Composites: A Review of Recent Developments. *Compos. Sci. Technol.* **2000**, *60*, 2037–2055. [[CrossRef](#)]
40. Joyklad, P.; Yooprasertchai, E.; Wiwatrojanagul, P.; Chaiyasarn, K.; Ali, N.; Hussain, Q. Use of Natural and Synthetic Fiber-Reinforced Composites for Punching Shear of Flat Slabs: A Comparative Study. *Polymers* **2022**, *14*, 719. [[CrossRef](#)]
41. Rousakis, T.C. Inherent Seismic Resilience of RC Columns Externally Confined with Nonbonded Composite Ropes. *Compos. Part B Eng.* **2018**, *135*, 142–148. [[CrossRef](#)]
42. Rousakis, T.C. Reusable and Recyclable Nonbonded Composite Tapes and Ropes for Concrete Columns Confinement. *Compos. Part B Eng.* **2016**, *103*, 15–22. [[CrossRef](#)]
43. Hussain, Q.; Ruangrassamee, A.; Tangtermsirikul, S.; Joyklad, P. Behavior of Concrete Confined with Epoxy Bonded Fiber Ropes under Axial Load. *Constr. Build. Mater.* **2020**, *263*, 120093. [[CrossRef](#)]
44. Fragoudakis, R.; Gallagher, J.A.; Kim, V. A Computational Analysis of the Energy Harvested by Gfrp and Nfrp Laminated Beams Under Cyclic Loading. *Procedia Eng.* **2017**, *200*, 221–228. [[CrossRef](#)]
45. Ghalieh, L.; Awwad, E.; Saad, G.; Khatib, H.; Mabsout, M. Concrete Columns Wrapped with Hemp Fiber Reinforced Polymer—An Experimental Study. *Procedia Eng.* **2017**, *200*, 440–447. [[CrossRef](#)]
46. ASTM C1314-21; Standard Test Method for Compressive Strength of Masonry Prisms. ASTM International: West Conshohocken, PA, USA, 2021.
47. ASTM C140/C140M-22a; Standard Test Methods for Sampling and Testing Concrete Masonry Units and Related Units. ASTM International: West Conshohocken, PA, USA, 2022.
48. ASTM A931-18; Standard Test Method for Tension Testing of Wire Ropes and Strand. ASTM International: West Conshohocken, PA, USA, 2018.
49. ASTM E8/E8M-13; Standard Test Methods for Tension Testing of Metallic Materials. ASTM International: West Conshohocken, PA, USA, 2013.
50. Deng, J.; Zheng, Y.; Wang, Y.; Liu, T.; Li, H. Study on Axial Compressive Capacity of Frp-Confined Concrete-Filled Steel Tubes and Its Comparisons with Other Composite Structural Systems. *Int. J. Polym. Sci.* **2017**, *2017*, 6272754. [[CrossRef](#)]
51. Qi, Y.; Xie, L.; Bai, Y.; Liu, W.; Fang, H. Axial Compression Behaviours of Pultruded GFRP–Wood Composite Columns. *Sensors* **2019**, *19*, 755. [[CrossRef](#)]
52. Hussain, Q.; Ruangrassamee, A.; Tangtermsirikul, S.; Joyklad, P.; Wijeyewickrema, A.C. Low-Cost Fiber Rope Reinforced Polymer (FRRP) Confinement of Square Columns with Different Corner Radii. *Buildings* **2021**, *11*, 355. [[CrossRef](#)]
53. Shehata, I.A.E.M.; Carneiro, L.A.V.; Shehata, L.C.D. Strength of Short Concrete Columns Confined with CFRP Sheets. *Mater. Struct.* **2002**, *35*, 50–58. [[CrossRef](#)]
54. Rodsin, K.; Hussain, Q.; Suparp, S.; Nawaz, A. Compressive behavior of extremely low strength concrete confined with low-cost glass FRP composites. *Case Stud. Constr. Mater.* **2020**, *13*, e00452. [[CrossRef](#)]
55. Richart, F.E.; Brandtzaeg, A.; Brown, R.L. A Study of the Failure of Concrete under Combined Compressive Stresses. *Bull. Eng. Exp. Stn.* **1928**, *26*, 12.
56. Miyauchi, K. Estimation of Strengthening Effects with Carbon Fiber Sheet for Concrete Column. In Proceedings of the 3rd International Symposium on Non-Metallic (FRP) Reinforcement for Concrete Structures, Sapporo, Japan, 14–16 October 1997; pp. 217–224.
57. Suparp, S.; Ali, N.; Al Zand, A.W.; Chaiyasarn, K.; Rashid, M.U.; Yooprasertchai, E.; Joyklad, P. Axial Load Enhancement of Lightweight Aggregate Concrete (LAC) Using Environmentally Sustainable Composites. *Buildings* **2022**, *12*, 851. [[CrossRef](#)]
58. Lam, L.; Hussain, Q.; Joyklad, P.; Pimanmas, A. Behavior of RC Deep Beams Strengthened in Shear Using Glass Fiber Reinforced Polymer with Mechanical Anchors. In Proceedings of the International Conference on Environment and Civil Engineering (ICEACE/2015), Pattaya, Thailand, 24 April 2015.
59. Ghernouti, Y.; Rabehi, B. FRP-Confined Short Concrete Columns under Compressive Loading: Experimental and Modeling Investigation. *J. Reinf. Plast. Compos.* **2010**, *30*, 241–255. [[CrossRef](#)]
60. Benzaid, R.; Mesbah, H. Nasr Eddine Chikh FRP-Confined Concrete Cylinders: Axial Compression Experiments and Strength Model. *J. Reinf. Plast. Compos.* **2010**, *29*, 2469–2488. [[CrossRef](#)]
61. Al-Salloum, Y.A. Compressive Strength Models of FRP-Confined Concrete. In Proceedings of the 1st Asia-Pacific Conference on FRP in Structures, APFIS 2007, Hong Kong, China, 12–14 December 2007; Volume 1, pp. 175–180.
62. Bisby, L.A.; Dent, A.J.S.; Green, M.F. Comparison of Confinement Models for Fiber-Reinforced Polymer-Wrapped Concrete. *ACI Struct. J.* **2005**, *102*, 62–72. [[CrossRef](#)]

63. Wu, H.-L.; Wang, Y.-F.; Yu, L.; Li, X.-R. Experimental and Computational Studies on High-Strength Concrete Circular Columns Confined by Aramid Fiber-Reinforced Polymer Sheets. *J. Compos. Constr.* **2009**, *13*, 125–134. [[CrossRef](#)]
64. Teng, J.G.; Huang, Y.L.; Lam, L.; Ye, L.P. Theoretical Model for Fiber-Reinforced Polymer-Confined Concrete. *J. Compos. Constr.* **2007**, *11*, 201–210. [[CrossRef](#)]
65. Ahmad, S.H.; Shah, S.P. Complete Triaxial Stress-Strain Curves for Concrete. *J. Struct. Div.* **1982**, *108*, 728–742. [[CrossRef](#)]
66. Hussain, Q.; Rattanapitikon, W.; Pimanmas, A. Axial Load Behavior of Circular and Square Concrete Columns Confined with Sprayed Fiber-Reinforced Polymer Composites. *Polym. Compos.* **2016**, *37*, 2557–2567. [[CrossRef](#)]
67. Karbhari, V.M.; Gao, Y. Composite Jacketed Concrete under Uniaxial Compression—Verification of Simple Design Equations. *J. Mater. Civ. Eng.* **1997**, *9*, 185–193. [[CrossRef](#)]
68. Samaan, M.; Mirmiran, A.; Shahawy, M. Model of Concrete Confined by Fiber Composites. *J. Struct. Eng.* **1998**, *124*, 1025–1031. [[CrossRef](#)]
69. Saafi, M.; Toutanji, H.A.; Li, Z. Behavior of Concrete Columns Confined with Fiber Reinforced Polymer Tubes. *ACI Mater. J.* **1999**, *96*, 500–509. [[CrossRef](#)]
70. Ilki, A.; Kumbasar, N. Behavior of Damaged and Un-Damaged Concrete Strengthened by Carbon Fiber Composite Sheets. *Int. J. Struct. Eng. Mech.* **2002**, *13*, 75–90. [[CrossRef](#)]
71. Spoelstra, M.R.; Monti, G. FRP-Confined Concrete Model. *J. Compos. Constr.* **1999**, *3*, 143–150. [[CrossRef](#)]
72. Mirmiran, A.; Shahawy, M. Behavior of Concrete Columns Confined by Fiber Composites. *J. Struct. Eng.* **1997**, *123*, 583–590. [[CrossRef](#)]
73. Pimanmas, A.; Hussain, Q.; Panyasirikhunawut, A.; Rattanapitikon, W. Axial Strength and Deformability of Concrete Confined with Natural Fibre-Reinforced Polymers. *Mag. Concr. Res.* **2018**, *71*, 55–70. [[CrossRef](#)]
74. Yan, L. Plain Concrete Cylinders and Beams Externally Strengthened with Natural Flax Fabric Reinforced Epoxy Composites. *Mater. Struct./Mater. Et Constr.* **2016**, *49*, 2083–2095. [[CrossRef](#)]
75. Pimanmas, A.; Saleem, S. Evaluation of Existing Stress–Strain Models and Modeling of PET FRP-Confined Concrete. *J. Mater. Civ. Eng.* **2019**, *31*, 04019303. [[CrossRef](#)]